RSC Advances

ROYAL SOCIETY OF CHEMISTRY

www.rsc.org/advances

RSC Advances

RSCPublishing

ARTICLE

Synthesis of zeolite from multilayer food packing and sugar cane bagasse ash for CO_2 adsorption

Murilo Pereira Moisés[a], Paula Pomaro de Almeida[a], Cleiser Thiago Pereira da Silva[a], Andrelson Wellington Rinaldi[a], Emerson Marcelo Girotto[a], Joziane Gimenes Meneguin[b], Pedro Augusto Arroyo[b], Ricardo Eugenio Bazan[c], Silvia Luciana Fávaro[d], Eduardo Radovanovic[a]*

The X/A zeolite crystals mixtures were synthesized using sugar cane bagasse ash (SCBA) as a silicon source and multilayer food packing (MFP) as an aluminum source under hydrothermal conditions at 80 °C for 79-296 hours. The silicon was extracted by alkaline fusion for 40 min at 550°C with an alkali/SCBA weight ratio of 1:1. The aluminum solution was obtained from MFP using NaOH 1M (3:1 water/acetone) solution. The synthesized zeolites were analyzed by XRD, FTIR, SEM, and BET. In the XRD results, most of the signals were indexed to zeolite X, and some signals were indexed to zeolite A. The vibration bands at region 1200-400cm^{-1} suggested the presence of the double-six-ring (D6R) zeolite X structure. The crystal morphology is characteristic of the zeolite X, and the specific area found by the BET method was 810.47 m^2/g. The zeolite with the higher specific area was applied in the CO_2 adsorption process until it reached 25 bar by the gravimetric method. The experimentally adsorbed amounts were adjusted with the Langmuir, Freundlich, and Toth models.

*Corresponding author. Tel.:55 44 3011 3653; fax: 55 44 3011 4125.
E-mail address: eradovanovic@uem.br (Eduardo Radovanovic)

Introduction

Zeolites are aluminosilicates of the alkaline and alkaline-earth metals with porous framework structures of corner-sharing SiO_4 and AlO_4 tetrahedral. Many industries use these materials, and decreasing production costs are relevant. One of the promising strategies to prepare zeolites at a low cost is to replace commercial chemicals with waste products as the starting precursor.[1] The disposal of large amounts of sugarcane bagasse ash and multilayer food packing has become a serious environmental problem. However, these solid wastes can be used in the zeolite synthesis process.

Sugar cane bagasse is a hazardous solid waste generated in large amounts in sugar mills. Combustion of sugar cane bagasse in boilers, used for steam and electricity generation, produces a great amount of another solid waste, denominated sugar cane bagasse ash (SCBA).[2] Employing this quartz-abundant waste as a silicon source can avoid its accumulation.[3]

The food packaging industry needs to develop multilayer films containing different polymers. Multilayer films may be manufactured by lamination or co-extrusion. These physical processes combine polymers into a film with special chemical, physical, and mechanical properties.[4,5] Another material that is used in these packages is aluminum, which protects food from the effects of sunlight and ultraviolet radiation.[6] A single medium-sized food packaging factory, for instance, produces about 8 tons monthly of parings of multilayer films containing aluminum. These films are gathered in the factory or turned into waste. Thus, the future of multilayer packages has become a great environmental concern.

Many researchers have used waste as a low-cost source of silicon and aluminium to produce zeolites. Different types of zeolites such as X,[7-9] ZSM-5,[10] hydroxysodalite,[7,11] Na-P1,[12,13] and zeolite A[3,14] were synthesized through many methods. Considering this, zeolite synthesis using solid waste as aluminium and silicon sources is a promising technique to recycle these wastes. This green strategy has received extensive attention over the last decade.

On the other hand, greenhouse gases are considered the cause of the global temperature increase, and this has attracted attention to the need to develop strategies to decrease carbon dioxide (CO_2) emissions.[15] The most commonly used techniques for CO_2 capture and separation from fuel gases include the ammonium absorption process,[16] dual-alkali absorption,[17] the membrane separation process,[18,19] and

adsorption on solid adsorbents.[20-24] Intense research is currently focused on the design of new and effective CO_2 adsorbents. The main challenge for greenhouse gas adsorption is to find a way to decrease the cost of the process and to make it more attractive than other market technologies. Therefore, CO_2 capture based on cheap technology with great potential for reducing the global cost of the sorbents is a very promising alternative for the future.[25,26]

One of the promising strategies to prepare low-cost sorbents is the replacement of commercial chemicals with waste products as the starting precursor.[27] Furthermore, the disposal of large amounts of sugar cane bagasse ash and multilayer food packing has become a serious environmental problem. Considering this, zeolite synthesis can be adopted as a promising technique for recycling these wastes and has received extensive attention over the last decade.

The purpose of this study was to synthesize zeolite using SCBA as a silicon source and MFP as an aluminum source and apply this green, low-cost zeolite in the CO_2 adsorption process by the gravimetric method at high pressure. This research demonstrates the potential of SCBA and MFP extract to be used as a reliable silica and aluminum source for preparing zeolites for CO_2 capture.

Experimental

Zeolite synthesis: The sugar cane bagasse ash (SCBA) was collected from the sugar cane industry located in the region of Maringá City, Paraná, Brazil. We placed the quartz material in a horizontal furnace and heated it in air at 20 ^oC/min from room temperature to 600°C and kept it for 4 h (SCBA600). Previous work has shown the characterization of these materials.[3] The silicon solution from SCBA was obtained via alkaline fusion treatment with NaOH at 773 K and a molar ratio of 1:1.5 (SCBA:NaOH) for 40 minutes. The solid resultant was diluted using distilled water (solution 1). The multilayer food packing was obtained from Inovaflex Rótulos e Etiquetas (Maringá, PR – Brazil). The parings of multilayer film containing 19±1.0 wt% of PET, 47 ± 1.0 wt% of PE, and 34 ± 1.0 wt% of Al were cut to 20×30 mm. Treating MFP with NaOH yielded the aluminum solution 1 mol/L (3:1 water/acetone) after 24 hours. After silicon and aluminum extraction, both solutions were mixed in the molar ratio $1SiO_2{:}0.4Al_2O_3{:}3.3Na_2O{:}173.8H_2O$. We transferred the mixture (2.0 L) to 10 polypropylene reactors (0.2 L each) and kept them at 80 °C for different crystallization periods (79, 121, 149, 163, 212, 235, 247, 272, 284, and 296 hours). Then, the solid was separated by filtration, washed with distilled water, and dried overnight at 100 °C.

Characterization: The zeolites were characterized by Fourier transform infrared spectrometry (Bomem-Michelson MB-100 with a resolution of 4 cm^{-1} using a KBr disc method). XRD analysis (Shimadzu, model XRD-6000 X-ray operated at 40 kV and 40mA, with Cu Kα (1,54Å) as the radiation source, diffraction angle - 2Θ - in the range 4^o - 60^o). The relative crystallinity was calculated using the area of diffraction signals localized in 2Θ = 6, 10 15, 23, 26, and 31^o. Scanning electron microscopy (SEM) (Shimadzu SSX-550 Superscan) characterized the morphology and the N_2 adsorption/desorption isotherm at 77 K (ASAP 2020 – Micromeritcs).

CO_2 adsorption: Adsorption equilibrium studies were performed with zeolite synthesized for 149 hours due to its higher specific surface area. The mass measurement was achieved using a magnetic suspension balance from Rubotherm (Bochum, Germany). The adsorbent was degassed in situ at 573 K until no mass variation was observed. Soon after, the measuring chamber was cooled down to the experiment temperature (298 K), and the gas pressure (CO_2) was increased stepwise (until 25 bar). The mass variation at equilibrium (m) was recorded for each pressure step. For the selected sample, a previous experiment with helium was carried out to determine the specific volume of the solid phase and the sample container volume, characteristic of the suspended parts inside the chamber. The sum of these volumes was used to account for the buoyancy effects on measurements with the adsorbed phase.

For a given gas pressure P, the adsorbed phase concentration may be calculated according to Equation 1[28-30]:

$$m_{ex}(P, T)=\Delta m(P,T)+[(V_b + V_s)\rho(P,T)] \quad (1)$$

where m_{ex} is the adsorption excess uptake (g/g sample), Δm is the mass difference sensed by the equipment (g/g sample), V_b is the volume of the balance-suspended components (cm^3), V_s is the specific volume of the sample (cm^3/g sample), ρ is the gas density (g/cm^3), P is the pressure (bar), and T is the temperature (K).

To clearly describe the CO_2 adsorption behavior on the synthesized zeolite, the Toth, Freundlich, and Langmuir models were used to fit the isotherm using the software Origin 7.0®. The description of adsorption models and equations was described in Supplementary Information.

Results and Discussion

Figure 1 displays the X-ray diffraction patterns of zeolite synthesis for each period of time. The diffraction peaks were indexed to zeolite type X and A as indicated in the figure. These zeolites exhibit Pm-3m and Fd-3 space groups, respectively (standard pattern number 71-0784 and 85-2064 - ICDD database and standard pattern of International Zeolite Association - IZA). After 79 h, X/A zeolite crystals mixtures were detected. Following the crystallization time, zeolitization increases until 149 h. After 149 h, crystallinity decreases, indicating an alkaline attack due to high crystallization time. This can be observed in the main signals to zeolite X (localized in 6, 10 15, 23, 26, and 31^o - 2 theta degrees). The materials with higher relative crystallinity were 149, 163, 212, and 247 h. However, the sample 247 h was ignorated to the adsorption test due to the long synthesis time. Available times verify Ostwald's rule[34]: the crystalline phase did not change successively, indicating that increasing time would not obtain pure-phase zeolite X.

Insert fig. 1

Figure 2 presents the FTIR spectra of the zeolites as a function of the hydrothermal process period. Peaks in the lattice region of 1200–400 cm^{-1} suggest the existence of zeolite X. The spectrum of X zeolite illustrates the presence of absorptions at 458, 559, 666, 746, and 974 $cm.^{-1}$ The 974 cm^{-1} band is due to the Si–O–Al asymmetric stretching vibration mode of T–O bonds, (where T = Si or Al). The band at 746 cm^{-1} is due to the S4R T–O–T symmetric stretching, while the absorption at 559 cm^{-1} is attributed to D6R T–O–T symmetric stretching and is very close to the external vibration of double four-rings (D4R) in the zeolite A framework localized at 557 $cm.^{-1}$ The two bands at 666 and 458 $cm^{-1}$are assigned to the Si–O–Al symmetric stretching and S4R symmetric bending modes, respectively. This band is slightly shifted and sharpens as the amorphous material transforms to crystalline zeolite. These results agree well with XRD and microscopy results. The OH band, related to deformational vibrations of adsorbed water molecules in zeolite channels, also appeared at about 1655 $cm.^{-1}$ [36]

RSC Advances ARTICLE

Insert fig. 2

The SEM observations in Figure 3 surveyed the external morphology of synthesized zeolites in different periods. A well-defined octahedral morphology is typical of zeolite X[7-9] and appeared in hydrothermal synthesis at 79 hours. After 212 h, the corrosion surface set in, indicating an alkaline attack on the surface due to the high crystallization time. This evidence corroborates the XRD and FTIR results.

Insert fig. 3

The textural properties were determined using BET, t-plot, and Dubinin-Radushkevich methods.[37] The specific surface area was used only for an internal comparison of the samples. The BET method obtained the total specific surface areas (we chose the linear region in the range of $0.004 < P/P0 < 0.04$), which were 810.47 m^2/g, 767.38 m^2/g, and 757.20 m^2/g to materials 149 h, 163 h, and 212 h, respectively, whereas the micropore areas determined by the t-plot method were 808.22 m^2/g, 764.01 m^2/g, and 755.41 m^2/g, indicating that these materials are priority microporous. This fact is also clearly using an internal comparison between the micropore and the total pore volumes determined by the t-plot, Dubinin-Radushkevich (DR), and BET methods (t-plot: 0.3062 cm^3/g, 0.2870 cm^3/g, and 0.2840 cm^3/g of micropores - DR: 0.3086 cm^3/g, 0.2906 cm^3/g. 0.2869 cm^3/g of micropores and total pore volume as determined by BET method were 0.3173 cm^3/g, 0.3026 cm^3/g, 0.2915 cm^3/g to materials 149 h, 163 h, and 212 h, respectively). The energy of nitrogen adsorption at 77 K was measured by the Dubinin-Radushkevich method presenting *ca.* 38 KJ/mol, indicating a physisorption process. The zeolite at 149 h exhibits the higher specific area and micropore volume, corroborating with XRD results that indicate that the 149 h material presented higher relative crystallinity. This fact points to a potential application of this green material because zeolite X has a large pore size (7.3 Å) and a high cation exchange capacity (5 $meqg^{-1}$), which make this zeolite an interesting molecular sieve and a high-cation exchange material.[14]

Insert fig. 4

Figure 5 shows the experimental CO_2 adsorption isotherm and the adjustment with the three models on the zeolite prepared for 149 h (Z-149) at 298 K at the pressures between 0 and 25 bar. It can be seen that the maximum adsorbed amounts of CO_2 on the zeolite sample is close to 7 mmol/g. However, this amount is achieved up to 3 bar pressure, indicating a fast saturation of the porous structure. This behavior at low pressure can be explained by the strong interaction between CO_2 molecules and the Z-149 surface. In fact, the high-energy sites are first occupied by CO_2 molecules [30]. The literature shows similar results for the amount of CO_2 adsorbed in porous materials.[38-44] Therefore, the results indicate that zeolite obtained from the sugar cane bagasse ash is a promising low-cost sorbent and has potential as an efficient gas-adsorption process.

Insert fig. 5

Table 1 shows the adjusted parameters of the Langmuir, Toth, and Freundlich models fitted on the CO_2 adsorption isotherm at 293 K. The CO_2 adsorption can be better fitted by the Toth adsorption equation. The Toth isotherm assumes that adsorption occurs on a heterogeneous surface containing sites with different energy and availability for adsorption.[28-30,32] In addition, when the affinity of the Toth constant *b* is larger, there is a stronger affinity of the adsorbate molecule toward the surface; in other words, the surface is covered by an organized layer of adsorbate molecules.

Insert table 1

In summary, the mechanism proposed for CO_2 adsorption in zeolite from solid waste indicates that this process mostly occurs in the cavities because this 149 h is predominantly a microporous material, due to the demonstrated micropore-specific area of the 808.22 m^2/g (determined by the t-plot method), while the total area was 810.47 m^2/g (determined by the BET method). Linear OCO-X^+ complexes are formed (X+ is the cation) that also involve the perturbation of Si–O–Al bonds according to Coluccia S. et al. (1999)[42] who obtained the formation of molecules linearly co-ordinated to X^+ cations (Lewis acidity) of the zeolitic supercages, and several different kinds of carbonate-like species form complex interactions, which was also reported by Martra, G. et al. (1999)[43] and Montanari, T. and Busca G. (2008).[44]

Conclusions

This work showed that sugar cane bagasse ash and multilayer food packing can be successfully used as raw material for the hydrothermal synthesis of green and low-cost zeolites, which have potential applications in the CO_2 adsorption process. This research contributes to materials and environmental science, suggesting the recycling of contaminant solid wastes generated in large amounts around the world. In fact, this reveals a new green and low-cost material for CO_2 adsorption, which is possibly doubly beneficial to environmental management because decreased contamination of hazardous solid wastes and greenhouse gas capture costs.

Acknowledgements

The authors acknowledge the financial support of CNPq. Murilo Pereira Moisés, Paula Pomaro de Almeida, and Cleiser Thiago Pereira da Silva would like to thank CNPq and Capes for the scholarships.

Notes and references

[a]Department of Chemistry, State University of Maringa, 5790 Colombo avenue, Zip Code 87020-900, Maringa, Parana, Brazil
[b]Department of Chemical Engineering, State University of Maringa, 5790 Colombo avenue, Zip Code 87020-900, Maringa, Parana, Brazil
[c]Department of Chemical Engineering, Federal University of Sao Carlos, km 235 Washington Luis highway, Sao Carlos, Sao Paulo, Brazil
[d]Department of Mechanical Engineering, State University of Maringa, 5790 Colombo avenue, Zip Code 87020-900, Maringa, Parana, Brazil

1 T. Witoon, and M. Chareonpanich, "Synthesis of hierarchical meso-macroporous silica monolith using chitosan as biotemplate and its application as polyethyleneimine support for CO2 capture," *Materials Letters,* vol. 81, pp. 181-184, Aug 15, 2012.
2 M. Balakrishnan, and V. S. Batra, "Valorization of solid waste in sugar factories with possible applications in India: A review," *Journal of Environmental Management,* vol. 92, no. 11, Nov, 2011.
3 M. P. Moisés *et al.*, "Synthesis of zeolite NaA from sugarcane bagasse ash," *Materials Letters,* vol. 108, pp. 243-246, Out, 2013.
4 A. Badeka *et al.*, "Physicochemical and mechanical properties of experimental coextruded food-packaging films containing a buried layer of recycled low-density polyethylene," *Journal of Agricultural and Food Chemistry,* vol. 51, no. 8, pp. 2426-2431, Apr, 2003.
5 S. Chytiri *et al.*, "Volatile and non-volatile radiolysis products in irradiated multilayer coextruded food-packaging films containing a buried layer of recycled low-

density polyethylene," *Food Additives and Contaminants,* vol. 22, no. 12, pp. 1264-1273, Dec, 2005.
6 A. K. Kulkarni, S. Daneshvarhosseini, and H. Yoshida, "Effective recovery of pure aluminum from waste composite laminates by sub- and super-critical water," *Journal of Supercritical Fluids,* vol. 55, no. 3, pp. 992-997, Jan, 2011.
7 H. Tanaka, and A. Fujii, "Effect of stirring on the dissolution of coal fly ash and synthesis of pure-form Na-A and -X zeolites by two-step process," *Advanced Powder Technology,* vol. 20, no. 5, Sep, 2009.
8 C. W. Purnomo, C. Salim, and H. Hinode, "Synthesis of pure Na-X and Na-A zeolite from bagasse fly ash," *Microporous and Mesoporous Materials,* vol. 162, Nov 1, 2012.
9 V. K. Jha *et al.*, "Zeolite formation from coal fly ash and heavy metal ion removal characteristics of thus-obtained Zeolite X in multi-metal systems," *Journal of Environmental Management,* vol. 90, no. 8, Jun, 2009.
10 M. Chareonpanich *et al.*, "Synthesis of ZSM-5 zeolite from lignite fly ash and rice husk ash," *Fuel Processing Technology,* vol. 85, no. 15, Oct 15, 2004.
11 N. Shigemoto, H. Hayashi, and K. Miyaura, "Selective formation of Na-X zeolite from coal fly-ash by fusion with sodium-hydroxide prior to hydrothermal reaction" *Journal of Materials Science,* vol. 28, no. 17, Sep 1, 1993.
12 M. Inada *et al.*, "Synthesis of zeolite from coal fly ashes with different silica-alumina composition," *Fuel,* vol. 84, no. 2-3, Jan-Feb, 2005.
13 G. G. Hollman, G. Steenbruggen, and M. Janssen-Jurkovicova, "A two-step process for the synthesis of zeolites from coal fly ash," *Fuel,* vol. 78, no. 10, Aug, 1999.
14 X. Querol *et al.*, "Synthesis of zeolites from fly ash at pilot plant scale. Examples of potential applications," *Fuel,* vol. 80, no. 6, May, 2001.
15 P. Nugent *et al.*, "Porous materials with optimal adsorption thermodynamics and kinetics for CO_2 separation," *Nature,* vol. 495, no. 7439, pp. 80-84, Mar, 2013.
16 J. T. Yeh *et al.*, "Semi-batch absorption and regeneration studies for CO_2 capture by aqueous ammonia," *Fuel Processing Technology,* vol. 86, no. 14-15, pp. 1533-1546, Oct, 2005.
17 H. P. Huang *et al.*, "Dual alkali approaches for the capture and separation of CO_2," *Energy & Fuels,* vol. 15, no. 2, pp. 263-268, Mar-Apr, 2001.
18 F. Ahmad *et al.*, "Process simulation and optimal design of membrane separation system for CO_2 capture from natural gas," *Computers & Chemical Engineering,* vol. 36, pp. 119-128, Jan 10, 2012.
19 L. Zhao *et al.*, "A parametric study of CO_2/N_2 gas separation membrane processes for post-combustion capture," *Journal of Membrane Science,* vol. 325, no. 1, pp. 284-294, Nov 15, 2008.
20 X. Yan, S. Komarneni, and Z. Yan, "CO_2 adsorption on Santa Barbara Amorphous-15 (SBA-15) and amine-modified Santa Barbara Amorphous-15 (SBA-15) with and without controlled microporosity," *Journal of Colloid and Interface Science,* vol. 390, pp. 217-224, Jan 15, 2013.
21 T. Witoon, and M. Chareonpanich, "Synthesis of hierarchical meso-macroporous silica monolith using chitosan as biotemplate and its application as polyethyleneimine support for CO_2 capture," *Materials Letters,* vol. 81, pp. 181-184, Aug 15, 2012.
22 J.-E. Park *et al.*, "CO_2 capture and MWCNTs synthesis using mesoporous silica and zeolite 13X collectively prepared from bottom ash," *Catalysis Today,* vol. 190, no. 1, pp. 15-22, Aug 1, 2012.
23 L. Liu *et al.*, "Zeolite synthesis from waste fly ash and its application in CO_2 capture from flue gas streams," *Adsorption-Journal of the International Adsorption Society,* vol. 17, no. 5, pp. 795-800, Oct, 2011.
24 C. Lu *et al.*, "Comparative study of CO_2 capture by carbon nanotubes, activated carbons, and zeolites," *Energy & Fuels,* vol. 22, no. 5, pp. 3050-3056, Sep-Oct, 2008.
25 M. Olivares-Marin *et al.*, "The influence of the precursor and synthesis method on the CO_2 capture capacity of carpet waste-based sorbents," *Journal of Environmental Management,* vol. 92, no. 10, pp. 2810-2817, Oct, 2011.
26 S. Sjostrom, and H. Krutka, "Evaluation of solid sorbents as a retrofit technology for CO_2 capture," *Fuel,* vol. 89, no. 6, pp. 1298-1306, 6//, 2010.
27 L. Y. Lin, and H. L. Bai, "Aerosol processing of low-cost mesoporous silica spherical particles from photonic industrial waste powder for CO_2 capture," *Chemical Engineering Journal,* vol. 197, pp. 215-222, Jul, 2012.
28 F. Dreisbach, A. H. R. Seif, and H. W. Losch, "Measuring techniques for gas-phase adsorption equilibria," *Chemie Ingenieur Technik,* vol. 74, no. 10, pp. 1353-1366, Oct, 2002.
29 F. Dreisbach, H. W. Losch, and P. Harting, "Highest pressure adsorption equilibria data: Measurement with magnetic suspension balance and analysis with a new adsorbent/adsorbate-volume," *Adsorption-Journal of the International Adsorption Society,* vol. 8, no. 2, pp. 95-109, Aug, 2002.
30 F. Dreisbach, R. Staudt, and J. U. Keller, "High pressure adsorption data of methane, nitrogen, carbon dioxide and their binary and ternary mixtures on activated carbon," *Adsorption-Journal of the International Adsorption Society,* vol. 5, no. 3, pp. 215-227, May, 1999.
31 K. V. Kumar *et al.*, "A site energy distribution function from Toth isotherm for adsorption of gases on heterogeneous surfaces," *Physical Chemistry Chemical Physics,* vol. 13, no. 13, pp. 5753-5759, 2011.
32 J. Toth, "Uniform Interpretation of gas-solid adsorption," *Advances in Colloid and Interface Science,* vol. 55, pp. 1-239, Mar, 1995.
33 X. Zhou *et al.*, "Thermodynamics for the adsorption of SO_2, NO and CO_2 from flue gas on activated carbon fiber," *Chemical Engineering Journal,* vol. 200, Aug 15, 2012.
34 I. LANGMUIR, "The Adsorption of gases on plane surfaces of glass, mica and platinum", 1918.
35 M. R. Anseau, "application of Ostwalds role to amorphous materials," *Physics Letters A,* vol. A 43, no. 1, 1973.
36 Z. T. Yao *et al.*, "Synthesis of zeolite Li-ABW from fly ash by fusion method," *Journal of Hazardous Materials,* vol. 170, no. 2-3, Oct 30, 2009.
37 Gregg, S. J.; Sing, K. S. W. Adsorption, Surface Area and Porosity; Academic Press: London, 1982.
37 S. Araki *et al.*, "Adsorption of carbon dioxide and nitrogen on zeolite rho prepared by hydrothermal synthesis using 18-crown-6 ether," *Journal of Colloid and Interface Science,* vol. 388, pp. 185-190, Dec 15, 2012.
38 G. Chandrasekar, W.-J. Son, and W.-S. Ahn, "Synthesis of mesoporous materials SBA-15 and CMK-3 from fly ash and their application for CO_2 adsorption," *Journal of Porous Materials,* vol. 16, no. 5, pp. 545-551, Oct, 2009.

39 K. S. Walton, M. B. Abney, and M. D. LeVan, "CO_2 adsorption in Y and X zeolites modified by alkali metal cation exchange," *Microporous and Mesoporous Materials,* vol. 91, no. 1-3, Apr 15, 2006.

40] M. Olivares-Marín *et al.*, "The influence of the precursor and synthesis method on the CO_2 capture capacity of carpet waste-based sorbents," *Journal of Environmental Management,* vol. 92, no. 10, pp. 2810-2817, 10, 2011.

41 M. Uibu, M. Uus, and R. Kuusik, "CO_2 mineral sequestration in oil-shale wastes from Estonian power production," *Journal of Environmental Management,* vol. 90, no. 2, pp. 1253-1260, 2, 2009.

42. S. Coluccia, L. Marchese, G. Martra, "Characterisation of microporous and mesoporous materials by the adsorption of molecular probes: FTIR and UV–Vis studies" Microporous and Mesoporous Materials vol.30, pp. 43–56, 1999.

43. G. Martra et al., "Acidic and basic sites in NaX and NaY faujasites investigated by NH3, CO2 and CO molecular probes" Res. Chem. Intermed., vol. 25, No. 1, pp. 77-93, 1999.

44. T. Montanari, and G. Busca, "On the mechanism of adsorption and separation of CO2 on LTA zeolites: An IR investigation," Vibrational Spectroscopy, vol. 46, no. 1, Jan 16, 2008.

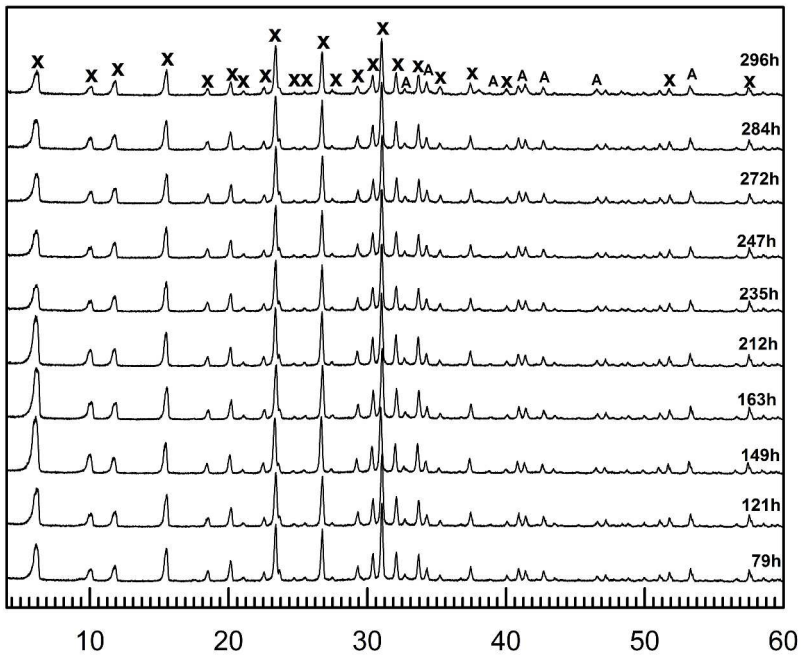

Figure 1. X-ray diffraction patterns of zeolite synthesis for each period of time.
1153x806mm (150 x 150 DPI)

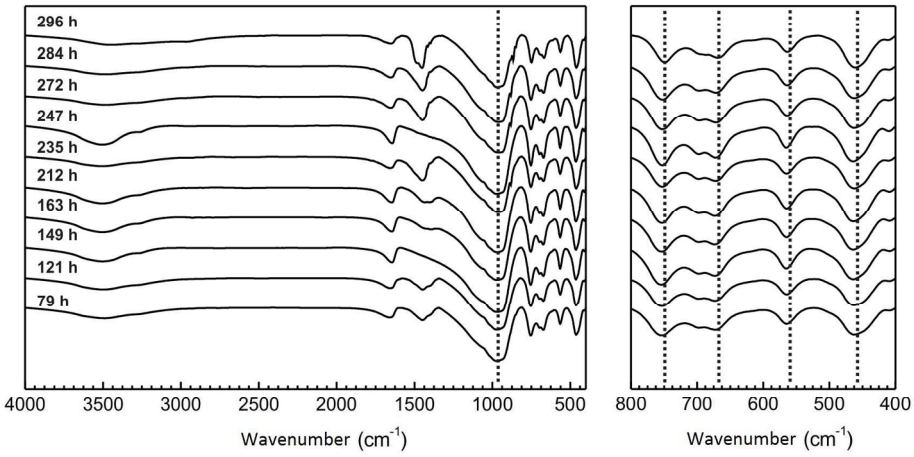

Figure 2. FTIR spectra of the zeolites as a function of the hydrothermal process period.
157x87mm (300 x 300 DPI)

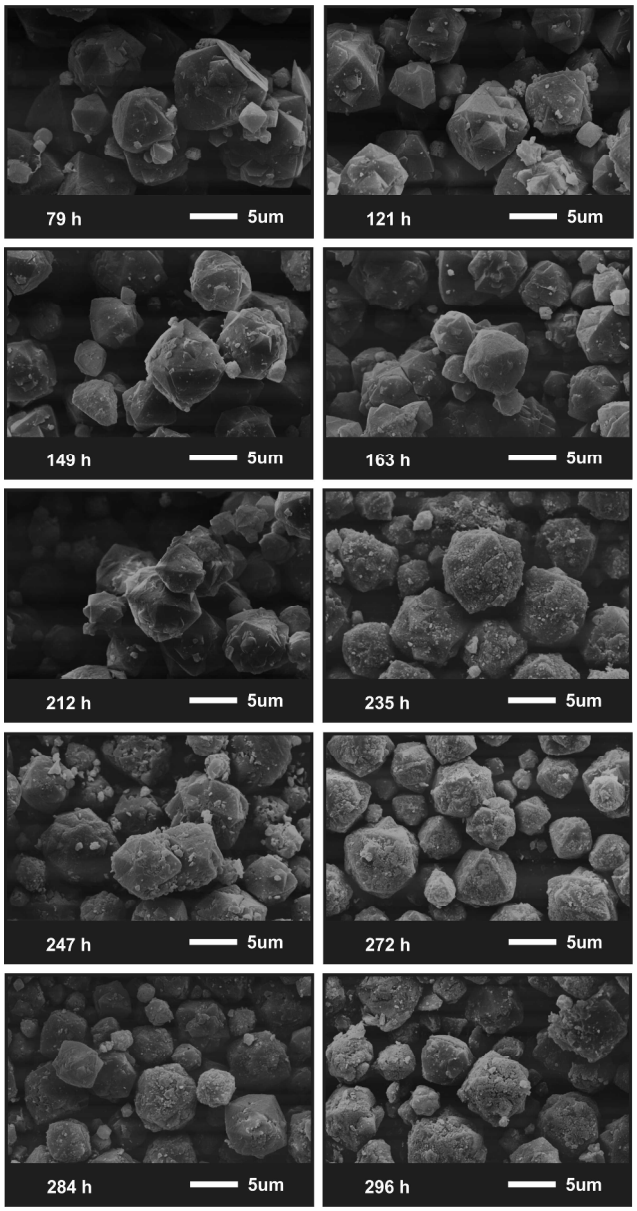

Figure 3. SEM images of zeolites.
201x384mm (300 x 300 DPI)

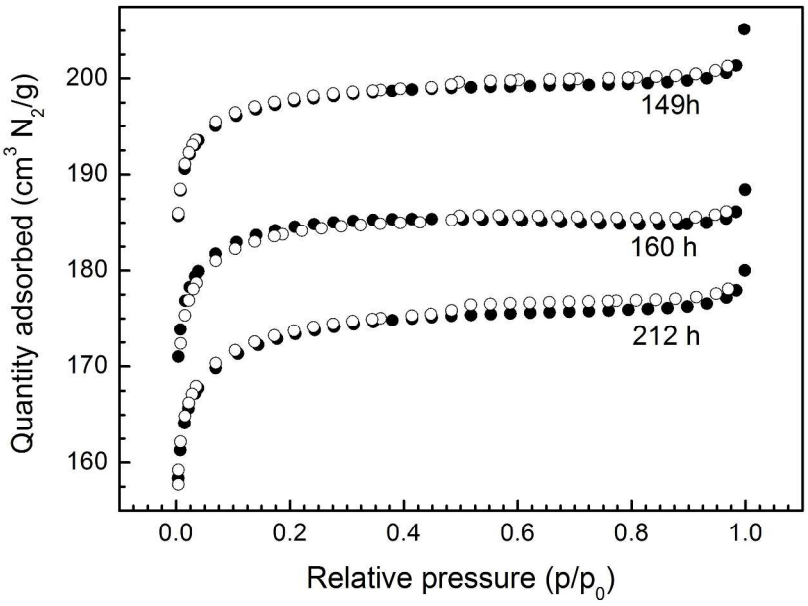

Figure 4. N2 adsorption–desorption isotherms at 77 K.
297x208mm (300 x 300 DPI)

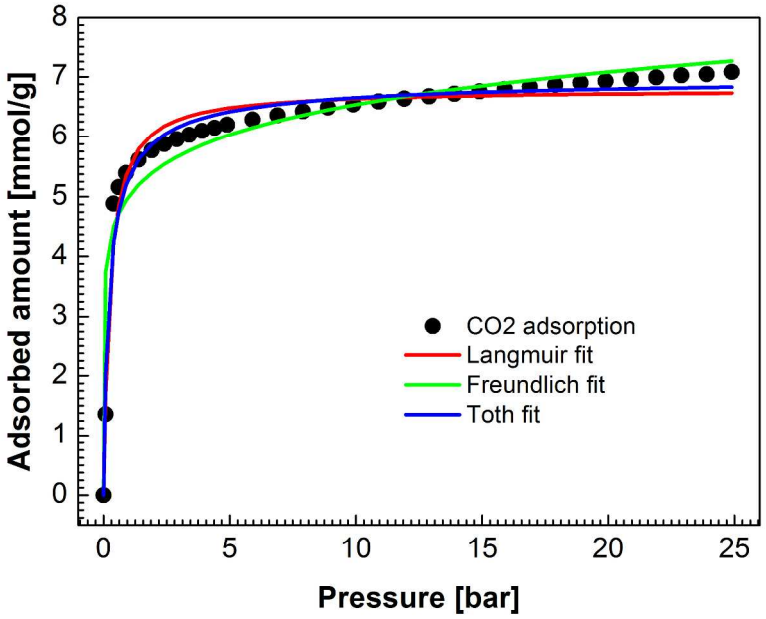

Figure 5.Experimental CO2 adsorption isotherm and the adjustment with the adsorption models on the zeolite prepared by 149h (Z-149) at 298 K.
297x210mm (300 x 300 DPI)

Table 1. Langmuir, Toth and Freundlich adjustments parameters of CO_2 isotherm at 293 K.

Toth				Freundlich			Langmuir		
qm (mmol/g)	b (bar^{-1})	n	r^2	n	k	r^2	qm (mmol/g)	b (bar^{-1})	r^2
7.01345	6.97833	0.75255	0.97622	8.64597	5.0041	0.90026	6.79188	4.16527	0.94069